AD-A128 714 REVIEW OF THE PROPAGATION OF INELASTIC PRESSURE WAVES IN SNOW(U) COLD REGIONS RESEARCH AND ENGINEERING LAB HANOVER NH D G ALBERT APR 83 CRREL-83-13 1/1

UNCLASSIFIED F/G 8/12 NL

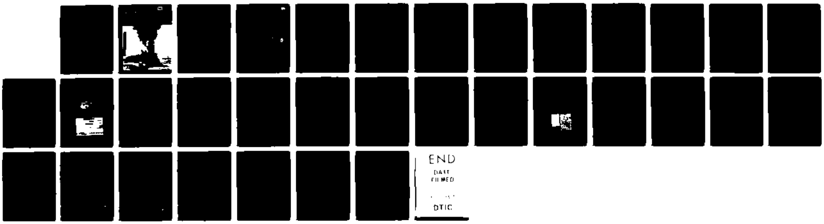

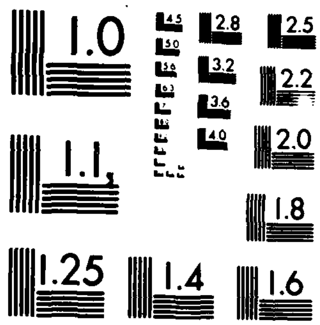

MICROCOPY RESOLUTION TEST CHART
NATIONAL BUREAU OF STANDARDS-1963-A

CRREL

REPORT 83-13

-AD A 128714

12

US Army Corps of Engineers
Cold Regions Research & Engineering Laboratory

Review of the propagation of inelastic pressure waves in snow

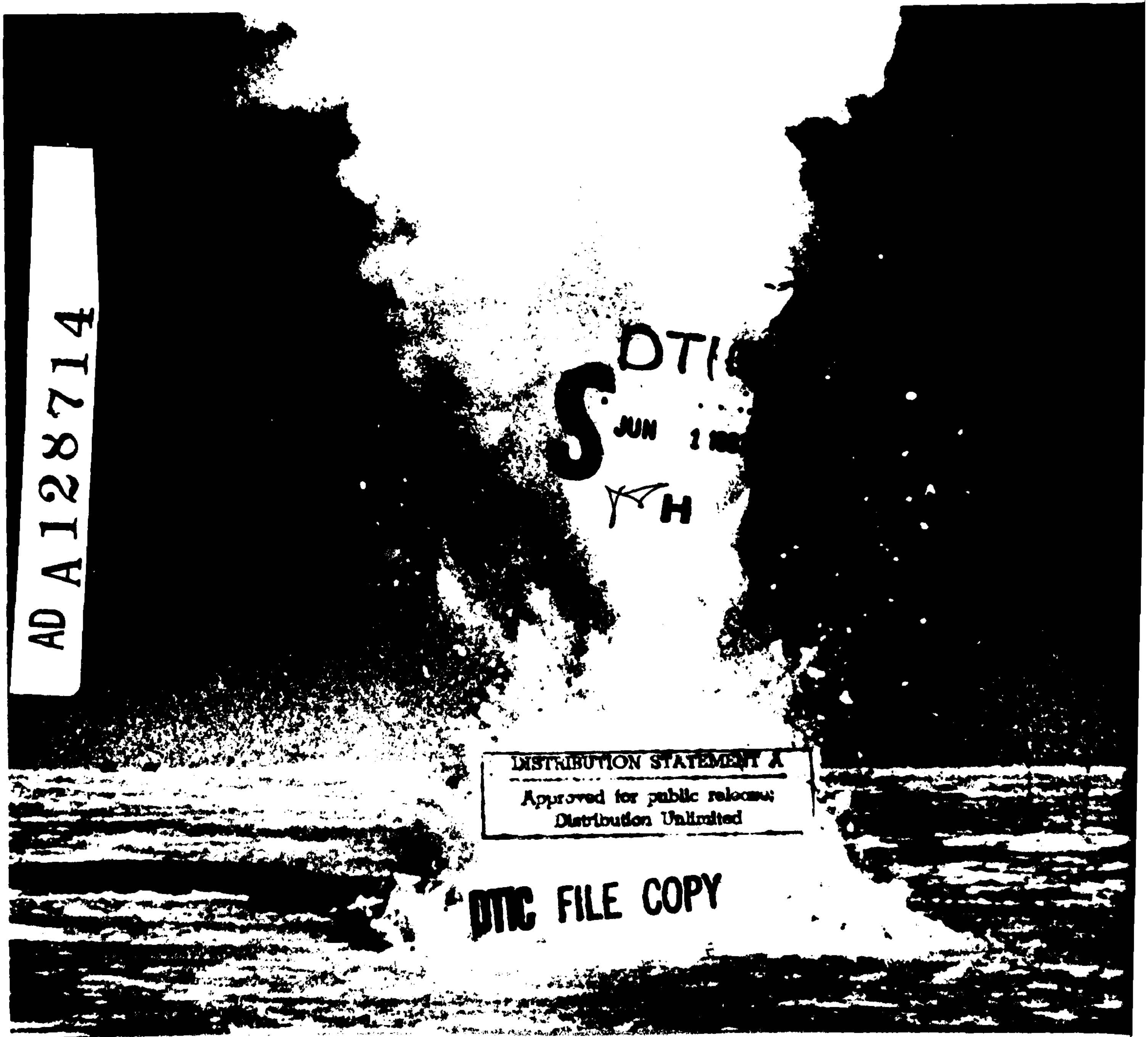

For conversion of SI metric units to U.S./British customary units of measurement consult ASTM Standard E380, Metric Practice Guide, *published by the American Society for Testing and Materials, 1916 Race St., Philadelphia, Pa. 19103.*

Cover: Detonation of an explosive charge in snow. Inelastic pressure waves produced by the explosion are rapidly attenuated as they propagate through the snow.

CRREL Report 83-13

April 1983

Review of the propagation of inelastic pressure waves in snow

Donald G. Albert

Prepared for
OFFICE OF THE CHIEF OF ENGINEERS
Approved for public release; distribution unlimited

Unclassified
SECURITY CLASSIFICATION OF THIS PAGE (When Data Entered)

REPORT DOCUMENTATION PAGE

READ INSTRUCTIONS BEFORE COMPLETING FORM

1. REPORT NUMBER
CRREL Report 83-13

2. GOVT ACCESSION NO.
A128714

3. RECIPIENT'S CATALOG NUMBER

4. TITLE (and Subtitle)
REVIEW OF THE PROPAGATION OF INELASTIC PRESSURE WAVES IN SNOW

5. TYPE OF REPORT & PERIOD COVERED

6. PERFORMING ORG. REPORT NUMBER

7. AUTHOR(s)
Donald G. Albert

8. CONTRACT OR GRANT NUMBER(s)

9. PERFORMING ORGANIZATION NAME AND ADDRESS
U.S. Army Cold Regions Research and Engineering Laboratory
Hanover, New Hampshire 03755

10. PROGRAM ELEMENT, PROJECT, TASK AREA & WORK UNIT NUMBERS
DA Project 4A762730AT42
Task A, Work Unit 015

11. CONTROLLING OFFICE NAME AND ADDRESS
Office of the Chief of Engineers
Washington, D.C. 20314

12. REPORT DATE
April 1983

13. NUMBER OF PAGES
33

14. MONITORING AGENCY NAME & ADDRESS (if different from Controlling Office)

15. SECURITY CLASS. (of this report)
Unclassified

15a. DECLASSIFICATION/DOWNGRADING SCHEDULE

16. DISTRIBUTION STATEMENT (of this Report)

Approved for public release; distribution unlimited.

17. DISTRIBUTION STATEMENT (of the abstract entered in Block 20, if different from Report)

18. SUPPLEMENTARY NOTES

19. KEY WORDS (Continue on reverse side if necessary and identify by block number)
Explosives
Fuel-air explosives
Inelastic pressure waves
Pressure signatures
Snow

20. ABSTRACT (Continue on reverse side if necessary and identify by block number)

A review on past experimental and theoretical work indicates a need for additional experimentation to charcterize the response of snow to inelastic pressure waves. Pressure data from previously conducted explosion tests are analyzed to estimate the elastic limit of snow of 400-kg m^{-3} density to be about 36 kPa. This pressure corresponds to a scaled distance of 1.6 m $kg^{-1/3}$ for charges fired beneath the surface of the snow, and to a scaled distance of 1.2 m $kg^{-1/3}$ for charges fired in the air. The effects of a snow cover on the method of clearing a minefield by using an explosive charge fired in the air above the snow surface are also discussed and recommendations are given for further work in this area. Explosive pressure data are used to estimate the maximum effective scaled radius for detonating

DD FORM 1473, 1 JAN 73 EDITION OF 1 NOV 65 IS OBSOLETE

Unclassified
SECURITY CLASSIFICATION OF THIS PAGE (When Data Entered)

20. Abstract (Cont'd).

buried mines at shallow depth to be 0.8 m $kg^{-1/3}$. Fuel-air explosive will increase this effective radius significantly because of the increase in the size of the source region.

PREFACE

This report was written by Donald G. Albert, Geophysicist, of the Geophysical Sciences Branch, Research Division, U.S. Army Cold Regions Research and Engineering Laboratory. This study was funded by DA Project 4A762730AT42, *Design, Construction and Operations Technology for Cold Regions*, Task A, *Cold Regions Military Operations*, Work Unit 015, *Mine and Countermine Performance in Cold Regions.*

The author would like to thank Dr. Malcolm Mellor and Michael Ferrick for technically reviewing this report, and Dr. Robert Brown for helpful comments.

The contents of this report are not to be used for advertising or promotional purposes. Citation of brand names does not constitute an official endorsement or approval of the use of such commercial products.

CONTENTS

ILLUSTRATIONS

Figure

TABLES

Table

LIST OF SYMBOLS

E	Young's modulus
G	shear modulus
ρ	density
Y	yield strength
P	pressure
u	particle velocity
U	wave velocity
F	energy
υ	Poisson's ratio
n	porosity = **pore volume** ÷ total volume of material
V	volume
P_{max}	maximum overpressure in the snow
λ	reduced distance = distance/(charge weight)$^{1/3}$
C_1, C_2, C_3	constants from empirical data
Y_0	yield stress for the matrix material
S_0	yield stress of ice
C, A	arbitrary constants (Brown 1979a)
D	principal difference of the rate of deformation tensor
α	ρ_{ice}/ρ
$\dot{\alpha}$	time derivative of α
ψ	acceleration term
J, ϕ	empirical constants in the work-hardening factor
$\bar{P}$	P/α
a_0	initial average pore radius
τ^2	$a_0{}^2 \rho_{ice}/3(\alpha_0-1)$
$f(\alpha)$	$(\alpha-1)^{-1/3} - \alpha^{-1/3}$
$H(\alpha)$	$\alpha \ln \alpha - (\alpha-1) \ln (\alpha-1)$
α_2	value of α at the transition from elastic to plastic deformation

REVIEW OF THE PROPAGATION OF INELASTIC PRESSURE WAVES IN SNOW

Donald G. Albert

INTRODUCTION

Objectives

This report reviews past work on propagation of inelastic pressure waves in snow. The primary aim of this review is to assess the effect of snow on schemes for clearing minefields with aerially detonated explosives. Snow is a very dissipative medium but its attenuative properties are difficult to measure accurately. Nevertheless, an evaluation of the attenuative behavior of snow would not only be applicable to clearing minefields, but also to the use of explosives for controlled avalanche release, snow plowing at high speed, and other cases where the dynamic properties of snow are important.

Background

When a force is applied to the free surface of a medium, the stress caused by the applied force is transmitted through the medium by propagating waves. The response of the material depends on the magnitude of the applied force and on the rate of application.

For small transient forces, the strain is usually proportional to the applied force. Such a material response is termed *elastic* and this response continues until the applied force exceeds a certain value known as the elastic or proportional limit (see Fig. 1). The linear relation between the stress (or applied force) and the resultant strain is known as Hooke's law. Two types of waves propagate in the medium: a longitudinal wave with a velocity of $\sqrt{E/\rho}$ and a shear wave of velocity $\sqrt{G/\rho}$, where ρ is the density, E is Young's modulus, and G is the shear modulus of the material (Love 1944).

If the applied force exceeds the proportional limit, the type of waves depends on the stress-strain response of the material. For a stress-strain curve such as I in Figure 1, high amplitude stress waves propagate faster than those of lower stresses. In such a material the wave front steepens as the wave propagates with a velocity that exceeds the elastic wave velocity. Such a wave is called a *shock* wave. If the stress-strain curve is like II in Figure 1, flow occurs when the proportional limit is exceeded, and an elastic wave follows a slower *plastic* wave through the material (Kolsky 1963).

The *yield strength* Y of a material is defined as the stress at a conventional amount of observed plastic strain (typically 0.2%). Two conditions are commonly used to describe the yielding of a material: the Tresca and the von Mises criteria. The Tresca yield criterion states that plastic flow occurs when the maximum shear stress in the material reaches a critical value. For the von Mises

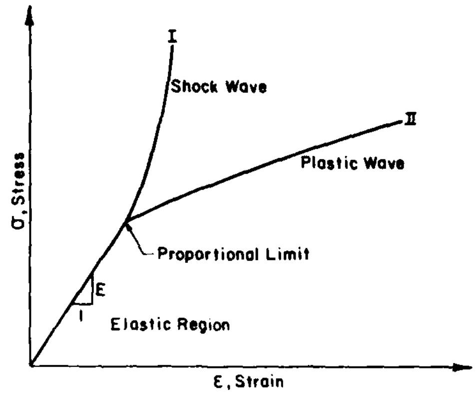

Figure 1. Stress-strain relation for a solid material.

criterion, plastic flow occurs when the strain energy of distortion reaches a critical value. The *ultimate strength* is defined as the stress at which the material fractures. These definitions are from Eisenberg (1980).

With these definitions a qualitative description of the response of a material caused by the impulsive force produced by an explosion can be given. The increase in pressure at the surface of the material (caused by contact between particles in the solid and in the air) is transmitted by a stress wave. If the stress is greater than the ultimate strength of the material, fracturing occurs. For smaller stresses, either a shock wave or a plastic and a precursor elastic wave propagate through the material, depending on the shape of the stress-strain curve (Fig. 1). For stresses lower than the proportional limit, elastic waves propagate through the medium. As the waves propagate, their amplitude is reduced by spherical divergence, the energy lost in fracturing and compressing the material, internal frictional forces, interaction between the pore air and the solid material, and so on. With increasing distance from the source of the wave, three distinct zones of material response are observed. Closest to the source is the fracture zone, then a zone of permanent deformation, and finally a zone of no deformation. The first two zones exist only if the initial stress is high enough to produce them. If the applied stress is transient (as in an explosion), waves due to unloading also propagate in the medium. The speed of these waves is determined by the properties of the material in the stressed state. For most materials supporting plastic waves, the velocity is higher for the unloading waves, and complicated variations in the wave amplitudes occur as the unloading wave catches and interferes with the initial or loading wave. Additional complications affecting wave amplitude arise in nonuniform media due to surface waves, reflections and refractions from interfaces, scattering, and diffraction.

To assess the effect of a snow cover on methods of clearing a minefield with explosives, predicting the amplitude of a wave at any distance from a known applied force is necessary. Amplitude predictions cannot be made without an accurate understanding of the dynamic behavior of snow. At present there are deficiencies in our knowledge of the response of snow to large stresses, as will be discussed in the next section.

Problems in describing the response of snow to an applied stress

Detailed knowledge of the dynamic behavior of snow has been hampered by experimental problems and theoretical gaps. Experimental work to characterize the dynamic properties of snow has been impeded by a number of factors. For example, natural snow has a wide variation in physical characteristics such as density, water content, and crystal structure. The variation in these characteristics will cause variatons in the dynamic response of different snow samples. Even with uniform samples, pressure measurements obtained in snow show large scatter. This scatter is related to experimental procedures such as gauge placement, the type of gauge used, and the variation in the snow characteristics themselves. A comparison of different experiments in an effort to estimate the general trends of snow behavior is therefore difficult. In addition, the high compressibility of snow makes preparation of natural snow samples troublesome because the structure of the snow is easily affected. Moreover, many measurement techniques used in shock tube experiments that depend on the electrical conductivity of the sample are eliminated by the insulating properties of snow.

Mellor (1975) reviewed the mechanical properties of snow and emphasized that its high compressibility makes it behave differently than most other materials, hampering both experimental and theoretical studies. His review gives a summary of the problems encountered in measurements of snow's behavior. In addition, Brown (personal communication)* has pointed out that snow will probably follow a more complicated relationship than either of the curves shown in Figure 1, especially for large compressive strains.

Theoretical work has been hampered by the lack of experimental data needed to characterize the general behavior of snow. The response of snow to an applied stress depends not only on the density, temperature, and other basic characteristics of the sample, but also on its strain and temperature history. The main theoretical problem is the development of an accurate description of the compaction of snow. Constitutive relations, which give the stress and strain of a material as a function of time in response to an applied stress, have recently been developed to explain the composition of porous metals (Carroll 1980). These relations show some promise for application to snow; however, the large difference in porosity between the two materials (20% for aluminum compared to 70% for snow of 300-kg m^{-3} density) indicates that the compaction mechanisms may be different.

Methods of determining the dynamic behavior of materials

For many dynamic problems, it is important to know how a material responds to the rapid application of a large force. Both theoretical and experimental methods give insight into material behavior, and past applications of these approaches will be briefly summarized in this section.

Theoretical models

Through the application of basic principles, information on the state of a material before and after the passage of a large amplitude shock or plastic wave can be determined. Let ρ be the density, P the pressure, u the particle velocity, U the wave velocity, and F the specific internal energy, with the subscripts 0 and 1 indicating values before and after the passage of the wave. Then, following Duvall and Fowles (1963), one can write the equations

$$\rho_0 U = \rho_1 (U - u_1) \tag{1}$$

$$P_1 - P_0 = \rho_0 U u_1 \tag{2}$$

$$P_1 u_1 = \tfrac{1}{2} \rho_0 U u_1^2 + \rho_0 U (F_1 - F_0) \tag{3}$$

corresponding to the conservation of mass, the conservation of momentum, and the conservation of energy. Using eq 1-3, the equation

$$F_1 - F_0 = \tfrac{1}{2} \left(\frac{1}{\rho_0} - \frac{1}{\rho_1} \right) (P_1 + P_0) \tag{4}$$

can be derived, relating the change in specific internal energy to the pressure and density before and after the passage of the wave. Equation 4 is known as the Rankine-Hugoniot equation. Equations 1-4, called the jump equations, have been widely used in reducing data from shock tube and other experiments.

*R.L. Brown, Montana State University, pers. comm. 1982.

The above equations rely upon the assumption that the material behaves as a fluid without shear forces or material rigidity. This hydrodynamic assumption is valid only when the wave amplitude is much greater than the strength of the material.

Many corrections to these equations have been made to allow them to be applied to real materials. For example, Fowles (1961) extended the above equations to the case of an elastic-plastic material at pressures on the order of the yield strength Y of the material. He investigated the case of a plane shock wave (one-dimensional strain) and used the von Mises yield criterion. For materials with properties independent of strain rate, the theory predicted that the pressure after the passage of a shock wave would be higher by an additional increment of $2Y/3$ above the stress required in the hydrostatic case to cause the same amount of compression. The shock was predicted to have a two-wave structure, composed of an elastic wave followed by a plastic wave. The theoretical amplitude of the elastic wave is $Y(1-\upsilon)/(1-2\upsilon)$, where υ is Poisson's ratio. Fowles (1961) reported measurements which confirmed this theory for aluminum.

Carroll and Holt (1972) developed a model of dynamic pore-collapse, the spherical pore model, which could be used to theoretically calculate stress wave propagation parameters and pressure-volume relations in porous materials. The model was later extended (Carroll and Holt 1973) to include the effects of shear stresses, viscosity, and work hardening. Extensions to the theory are continuing (e.g. Swegle 1980).

The spherical pore model makes a number of assumptions about the nature of the porous material (Carroll 1980). It assumes that the substance consists of a solid matrix material containing spherical pores and that these pores are isolated from each other. By assuming a yield condition for the solid matrix, the theory can be used to derive a relation between the applied pressure P and the porosity n, the pore volume divided by the total volume of the material. For porous metals, the matrix material is assumed to be an ideally plastic substance obeying either the von Mises or the Tresca yield condition, which are the same for this spherical geometry. When the applied pressure is high enough that only plastic deformation is occurring, the model predicts the following relation:

$$P = -\frac{2}{3} Y \ln n$$

where Y refers to the solid matrix. For porous rocks, a different yield condition is assumed and a different relation between P and n is found. The assumptions contained in the model, along with examples of its application to different substances, are discussed in a review paper by Carroll (1980).

A theory based on spheres (grains) in contact with each other is discussed in a review by Schatz (1976). This model assumes that the spheres yield plastically under an applied pressure. From the geometry of the model (shown in Fig. 2), Schatz finds that

$$\frac{\Delta V}{V} = 3\left(\frac{GP}{\pi Y} + 1\right) - 2\left(\frac{4P}{\pi Y} + 1\right)^{3/2} - 1$$

where $\Delta V/V$ is the change in volume per unit volume resulting from the applied pressure P. Since the model does not assume that the pores are isolated, it can be applied to materials with high porosities. Schatz (1976) also discusses work done in adapting the model to nonspherical grains.

Although the above models require experimental data to determine the values of some parameters, they have two advantages over purely empirical models. First, they offer an explanation for the mechanical process of compaction. Second, the model parameters are not arbitrary but have physical meaning and can be measured by specific tests.

Experimental methods

Experimental techniques for measuring shock wave properties of hydrodynamic materials are summarized by Duvall and Fowles (1963). Instrumentation and accuracy have been continually

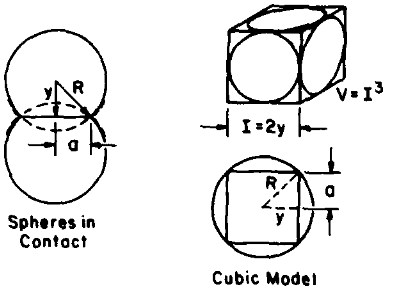

Figure 2. Geometry for the plastic deformation of equal spheres in simple cubic packing. As an external pressure is applied, the spheres deform plastically along a circular area of radius α, while the remaining portion of the sphere (of radius R) is undeformed (after Schatz 1976). (Other symbols give values used in the model).

improved, but the general procedure remains unchanged. A flat plate is accelerated (by means of explosives or a gas gun) and strikes a target containing a sample of the material to be measured. Either the impact is flat (the usual procedure), producing a plane wave in the material, or oblique, allowing the behavior at more than one stress value to be measured. The purpose of the experiment is to measure any two of the parameters in eq 1 and 2, allowing the other values to be calculated. The shock wave velocity U can be measured by timing the transit of the wave through the sample of known thickness. The particle velocity u can be measured by observing the motion of the free surface of the sample, but this method requires some approximation since the free surface velocity is influenced by reflections back into the sample. Electrical methods of determining accurate velocities have been used but would be difficult with snow since it is an insulator. Duvall and Fowles (1963) discuss these and other experimental methods in detail.

Seaman (1976) has reviewed the experimental methods for determining the constitutive relations of porous materials. The technique that appears to be best suited to investigating materials with high initial porosity (such as snow) involves the use of multiple imbedded stress or particle velocity gauges. After an impact into the target, records are obtained that show the propagation of the compaction and unloading waves as they pass through the target material. The main problem with this method is that it requires very accurate gauge calibration, gauge placement, and timing. If good data can be obtained, however, the method provides a complete record of the dynamic behavior of the material. The velocity of the waves, attenuation of the peak amplitude, and the stress-strain curves of the material can all be obtained from this method.

Seaman (1976) also discusses two other experimental techniques: the transmitted wave and the shock reverberation methods. These methods are much easier to perform, but have the disadvantage that only a very limited amount of data are obtained from each impact, so that many different samples are needed. Butcher et al. (1974) have applied these latter two methods to the study of porous aluminum. They compared their measurements to calculations using the spherical pore model and found qualitative agreement with the model. Butcher et al. (1974) also found that work-hardening effects increased the strength of the material at high strain rates so that the elastic precursor amplitude would be several times higher than the values predicted by Fowles' (1961) equations.

REVIEW OF PREVIOUS STUDIES ON SNOW

Experimental measurements on snow

Experimental studies of the compression of snow at a rate of 0.4 m s^{-1} (at strain rates from 1 to 10 s^{-1}) show that it behaves as a viscoplastic material and has a stress-strain behavior similar to that shown by curve II in Figure 1 (Abele and Gow 1976). For large applied stresses, snow will support an elastic and a plastic wave, but not a supersonic shock wave.

Laboratory measurements

Napadensky (1964) made the first attempt to measure the response of snow to a high speed impact in the laboratory. A metal plate was explosively accelerated and impacted into a snow sample. The wave and particle motion in the sample was observed using a streak camera to record the movement of lines painted on the snow surface. Impact velocities of 7.5 to 125 m s^{-1} were achieved, corresponding to pressures on the order of 0.6 to 20 MPa. The experiments were carried out on natural and processed Greenland snow with a density of 390 to 530 kg m^{-3}.

To reduce the data, Napadensky applied hydrodynamic equations similar to eq 1 and 2 to the double wave structure of the precursor elastic wave followed by the plastic wave. Unfortunately there were a number of experimental problems. The time resolution of the streak camera was not sufficient to accurately measure the velocity of the elastic precursor wave, which was instead estimated from other sources. The spatial resolution was not accurate enough to determine the particle

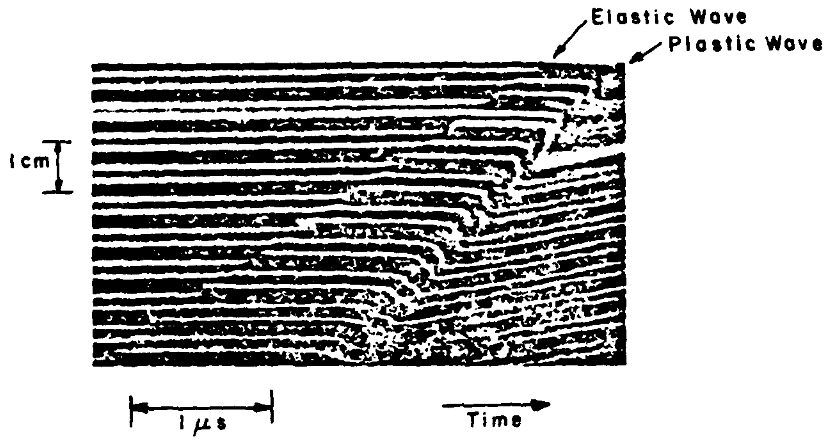

a. Hardened aluminum, reproduced from Fowles (1961).

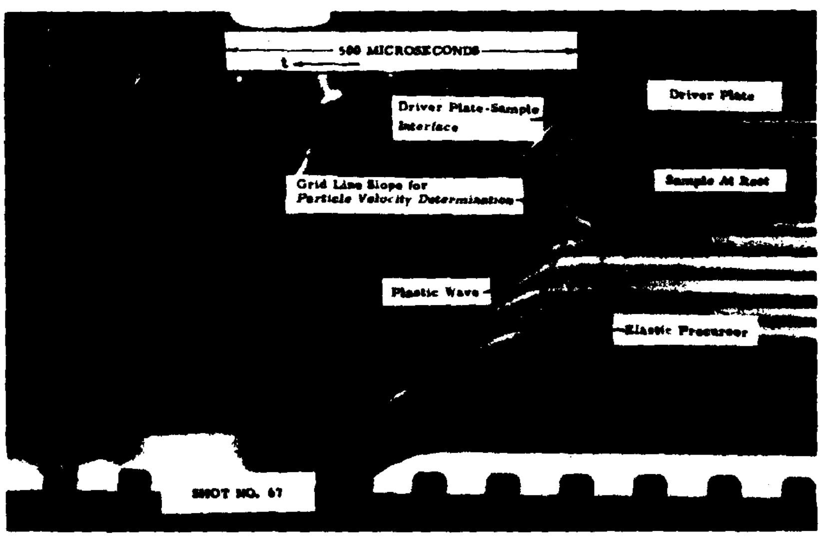

b. Snow, reproduced from Napadensky (1964).

Figure 3. Streak camera photographs of shock wave compression.

velocity after the passage of the elastic wave. An attempt was made to improve the accuracy of the experiment to resolve both waves (Napadensky 1965), but this effort was not successful.

In light of the results of Fowles (1961), however, the elastic precursor wave does not appear to be of great importance for the pressure ranges measured by Napadensky. A qualitative assessment of the importance of the elastic precursor wave can be obtained by examining Figure 3, in which streak camera records from Fowles (1961) and from Napadensky (1964) are shown. The two-wave structure is obvious in Fowles' data, but is much less so in Napadensky's. A general graph of snow's expected behavior in one-dimensional strain is shown in Figure 4.

Figure 5 presents the plastic wave velocity vs. particle velocity as measured by Napadensky (1964). The figure shows that the particle velocity generally increases with the plastic wave velocity. The scatter in the data is rather large: about 30 m s^{-1} for each velocity measurement. This scatter could be reduced with modern experimental equipment if these experiments were repeated. A serious shortcoming in Napadensky's data reduction procedures was the use of hydrodynamic equations to calculate the final density of the snow and the pressured differences across the wavefronts. These equations assume that all of the energy involved is used to compress the snow uniformly. For unconfined snow samples, uniaxial compression rarely results in densities greater than about 600 kg m^{-3}. At higher pressures, after this density is reached, cracking occurs and the snow crumbles and is pushed aside (Mellor 1965). Energy is used to form these cracks, but the hydrodynamic theory assumes that all of the energy is used only to compress and compact the snow. The final density values calculated by Napadensky are therefore unrealistically high. Values greater than 1000 kg m^{-3} were reported for some tests with pressures always less than 20 MPa. If these tests

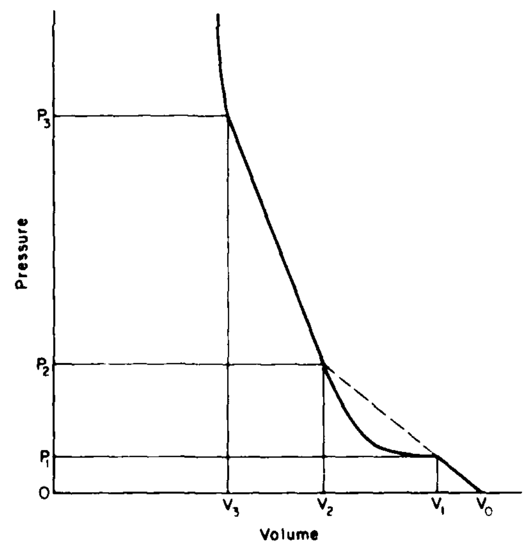

Figure 4. General pressure vs volume graph for snow. Subscripts 1 and 3 refer to the elastic limit and the volume of closest packing of the ice grains, respectively. At pressures > P_3, fracturing occurs. For P < P_1 only elastic waves exist. For P_1 < P < P_2, an elastic wave followed by a plastic wave will exist. For P > P_2, only a plastic wave will exist.

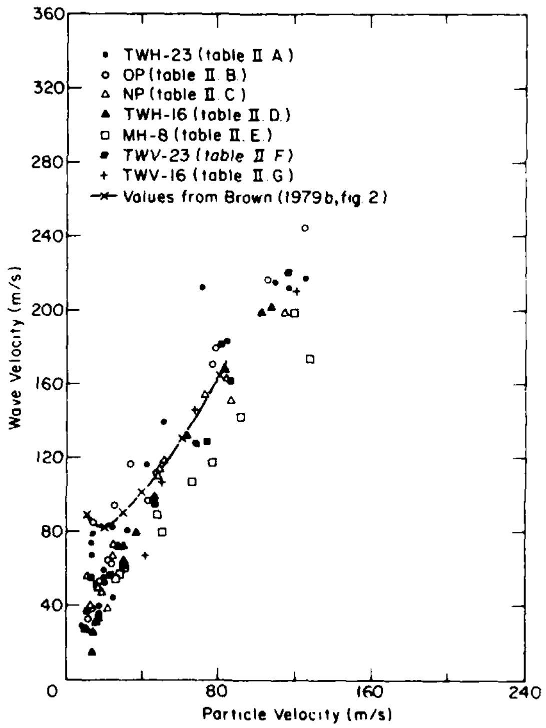

Figure 5. Plastic wave velocity vs particle velocity for Greenland snow. Comparison of Napadensky's (1964) actual data with Brown's (1980a) predicted values (see Theoretical Studies *below). Modified from Brown (1980a).*

are repeated, then a stop should be used as suggested by Napadensky (1964) to catch the driver plate of the test machine so that the sample can be recovered and the final compaction measured; in addition, pressure sensors should be used to provide an additional check on the results.

Napadensky's (1964) data remain the most extensive available today on the dynamic behavior of snow. However, the methods used to convert the particle and plastic wave velocities to final densities and pressures are in error because the hydrodynamic theory does not apply to snow at high strain rates. Direct measurements of these parameters are still needed for snow.

A second study of a plastic wave propagating in snow as a result of an impact was reported by Sato and Wakahama (1976). The experiment used a 1-kg weight dropped from heights of up to 2 m onto the snow sample, so that the impact speed was limited to a maximum of 5 m s^{-1}. They observed the motion of lines painted on the edge of the snow sample using high-speed motion pictures at 4200 frames/s, which allowed them to measure the plastic wave velocity and particle velocity. In addition, a pressure transducer embedded in the snow was used to measure the arrival time and pressure of the plastic wave. The elastic wave could not be resolved in this experiment.

Sato and Wakahama assumed that the final density of the snow could not exceed 600 kg m^{-3}. For cases where the hydrodynamic equations predicted a higher final density, they predicted and observed that fractures would occur. Their results show that for a constant impact velocity of 4.3 m s^{-1}, the plastic wave velocity increases from 5 to 12 m s^{-1} with an increase in initial snow density from 100 to 400 kg m^{-3} as predicted by rearranging eq 1. They also examined thin sections of the samples after impact, and observed that the pore spaces between the grains were closed, but with little deformation of the grains themselves.

Using eq 2, Sato and Wakahama calculated values of 5 to 10 kPa for the pressure change across the wavefront, and they report measured values from the imbedded pressure transducer of 10 to 30 kPa. Not enough details are given to evaluate the three-fold difference between the calculated and observed values. The discrepancy could be due to an impedance mismatch between the snow and the pressure gauge, disregarding the pressure increase caused by the precursor elastic wave, or using the hydrodynamic theory outside its range of validity.

Smith (1969) attempted to measure the pressure-volume behavior of snow using a shock tube. However, the applied pressures were too low for a plastic wave to be formed. In addition, the shock wave velocities measured exceeded the elastic wave speed for most of the measurements, casting doubt upon the accuracy of the results.

Field measurements

In addition to the above laboratory experiments, a number of field studies of the effects of explosions on snow have been conducted. Many of these studies attempted to measure the attenuation of a blast wave with distance in the snow.

Poulter (1950) was the first to report that stronger elastic waves could be produced from a given charge size by firing it in the air rather than in snow. This conclusion was based on reflection amplitudes rather than pressure measurements.

Ingram and Strange (1958) presented some of the earliest pressure measurements in snow. They detonated 3.6-kg (8-lb) charges at mid-depth in a 1.2-m- (4-ft-) deep snowpack and measured the pressures in the snow with piezoresistive gauges. The density of the snow was 250 kg m^{-3} in the upper 0.5 m and 380 kg m^{-3} below that depth. Ingram and Strange's pressure data vary in amplitude by a factor of 2 to 5 over the five shots measured; in addition, the pressures for all but the closest measuring point were very low compared to the gauge range, suggesting inaccuracies. However, this appears to be the first attempt to measure the attenuative properties of snow. They found that the equation,

$$\log (P_{max}) = C_1 \log (\lambda) + C_2, \tag{6}$$

fit the averaged data with $C_1 = -2.59$ and $C_2 = -1.97$ where P_{max} is the maximum overpressure in the snow in lbf/in.^{2} and λ is the reduced distance (the distance from the charge divided by the cube root of the charge weight) in ft lb$^{-1/3}$. As is usual in explosion studies (Mellor 1965), distances are scaled by the cube root of charge weight, which is proportional to the energy yield, to remove the effects of charge size. Converting this equation to standard form gives

$$P_{max} = C_3 \lambda^{C_1} . \tag{7}$$

For Ingram and Strange's data, C_1 will have the same value as above and

$$C_3 = 10^{C_2} = 1.07 \times 10^{-2}.$$

In addition to the problem with the gauge range mentioned above, the data may not give the proper indication of the amount of attenuation caused by snow because the snow layer was so thin.

Similar experiments were repeated in Greenland to assess the effects of an air blast on a snow arch (Ingram 1960). However, the pressure gauges used appeared to have a rise time that was too slow for this type of measurement, and the data are questionable. Mellor (1965) gives a review of other early measurements (including those presented in Livingston 1968, discussed below).

Wisotski and Snyder (1966) also investigated the attenuation of blast pressures with distance traveled in a snowpack. They used pressure transducers of two types: paddle gauges and pencil gauges. There is significant scatter in the data, and there appear to be systematic differences between the response times and peak pressures measured with the two different types of gauges.

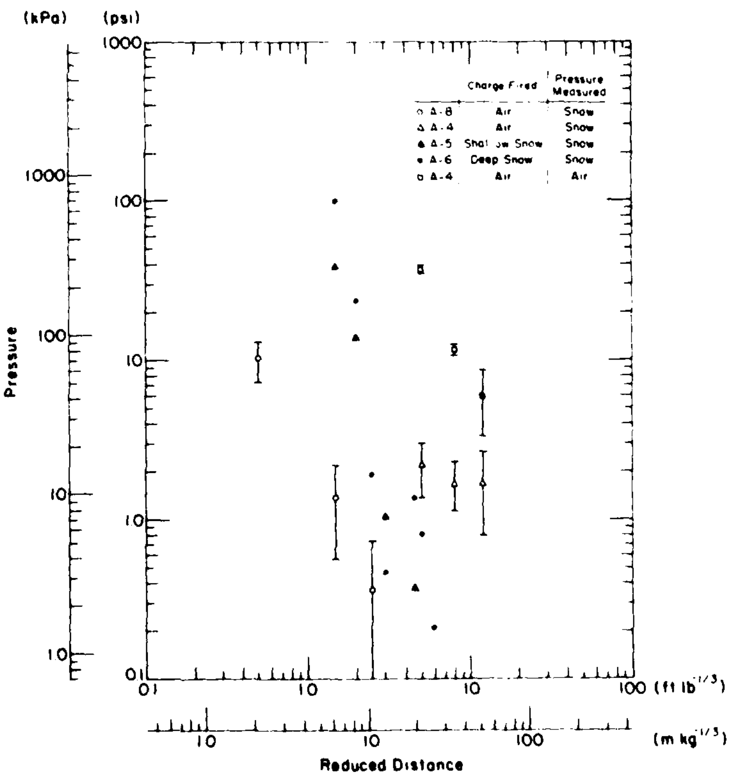

Figure 6. Logarithmic plot of maximum pressure vs reduced distance for explosions in and above seasonal snow (data from Wisotski and Snyder 1966).

Despite the above problems, Wisotski and Snyder conclude that, for a given distance from the charge, an explosion detonated in the air produces much higher pressures in the snowpack than an explosion detonated within the snow itself. Wisotski and Snyder postulate that this difference is because much of the energy of a charge exploded in the snow does work in vaporizing and melting the snow nearby, although Poulter (1950) had showed that very little snow is vaporized during explosions. Energy would also be used in forming the crater and the wave would be attenuated due to the greater losses caused by the snow itself. Average values of their data, compiled in Appendix A and shown in Figure 6, show that the peak pressure is indeed lower when the charge is fired in the snow, but only for distances greater than 1 m from the charge, i.e. in the *elastic* range. Closer to the shot, where deformation of the snow is occurring, peak pressures are higher for charges fired within the snow.

Joachim (1967) reported on measurements taken during air, surface, and subsurface blasts in Greenland. Accelerometers were used to record the motion at depth in the snow and pressure gauges were used to measure the pressure of the airblast. The travel times in the snow are in agreement with other measurements of elastic wave velocity, but no pressure measurements were made there.

Livingston (1968) reported on an extensive series of explosion tests conducted in Greenland in 1958. The primary emphasis of Livingston's report is on cratering, but 32 of the 141 shots were instrumented for pressure measurements. A few examples of the pressure data were presented, but no analysis was done. The pressure data are tabulated in Livingston (1964) and are reproduced in Appendix B.

Livingston's data can be used to derive an empirical equation for the maximum overpressure as a function of distance from a charge exploded in the snow. Since no significant differences were

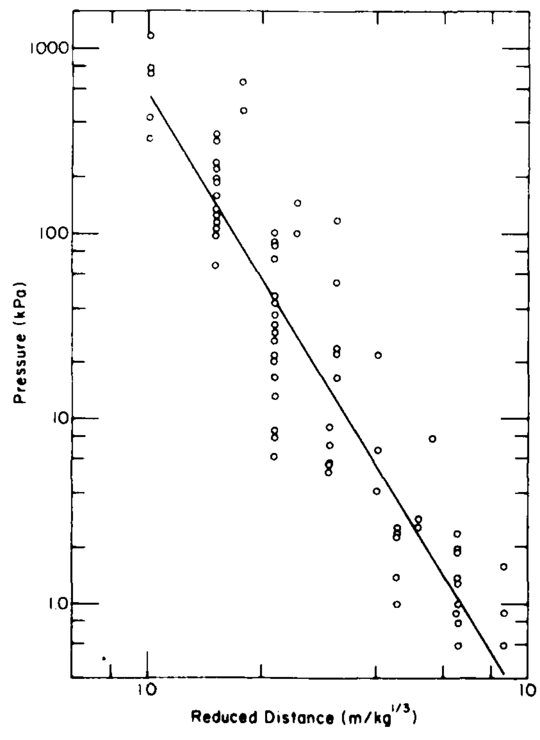

Figure 7. Graph of the log of maximum pressure vs log reduced distance for explosions in Greenland snow. Data from Livingston (1964) and reproduced in Appendix B.

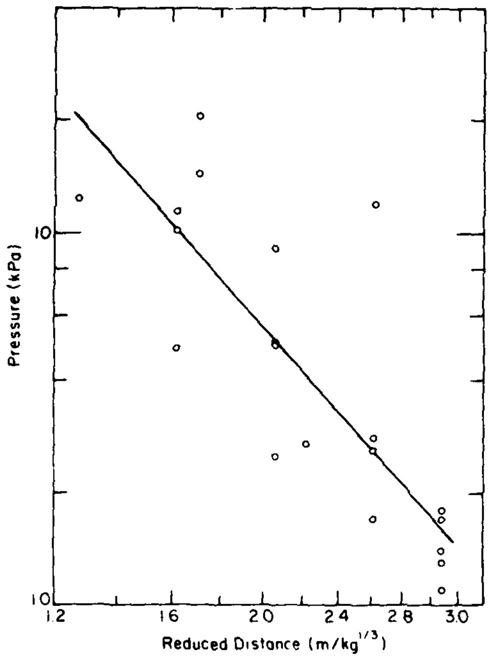

Figure 8. Graph of log maximum pressure vs log reduced distance for explosions above Greenland snow. Data from Livingston (1964) and reproduced in Appendix B.

found for different types of explosives (Atlas 60% gelatin, Atlas Coalite 75, and military explosive C-4), the data from all types are combined in the analysis. The data are plotted in Figure 7, along with a least-squares line fit to the data. The constants C_1 and C_3 of eq 7 are

$$C_1 = -3.33 \pm 0.16 \text{ and } C_3 = 550 \pm 39$$

the error bounds being one standard deviation. The data show an inverse cube decay. If the pressure is given in Pa and λ in m kg$^{-1/3}$, C_1 is unchanged and

$$C_3 = (1.74 \pm 0.08) \times 10^5 .$$

Data for shots fired in the air above the snow surface are shown in Figure 8.

Using the crater dimensions for these shots given in Livingston's (1968) appendix, the scaled true crater radius (for zone of total fragmentation) and scaled extreme rupture radius (for zones of plastic deformation) can be determined. These distances, along with the corresponding measured pressure values, are given in Table 1. The distance values are in agreement with Mellor's (1965) summary of the Livingston data and data from seasonal snow. The data show that a charge set off in the snow will produce higher overpressures for plastic waves than one set off in the air. The data also indicate that the maximum overpressure in the snow will be higher for shots fired in the snow than for shots fired above the snow surface. These results were obtained for fairly dense (300- to 400-kg m^{-3}) Greenland snow and apply only to stresses high enough to permanently deform the snow (pressures of 10 to 30 kPa and higher).

Gubler (1977) reported on measurements of explosions on a seasonal snow cover 1 to 2 m deep (density 150 to 500 kg m^{-3}). He measured the air pressure at the snow surface and acceleration within the snow as the charge location, size, and type were varied. The actual data are not given but it appears that the relations he derives are valid only within the elastic region. Gubler measured a higher particle velocity at the snow's surface by a factor of 10 for charges fired above, rather than

Table 1. Pressures and scaled distances from Livingston's (1964, 1968) data.

	True crater zone				Extreme rupture zone			
	Scaled radius		Pressure		Scaled radius		Pressure	
*Charge location**	*(ft lb$^{-1/3}$)*	*(m kg$^{-1/3}$)*	*(psi)*	*(kPa)*	*(ft lb$^{-1/3}$)*	*(m kg$^{-1/3}$)*	*(psi)*	*(kPa)*
Snow	3.39 ± 0.22	1.34 ± 0.09	9.4	64.9	4.07 ± 0.13	1.61 ± 0.05	5.1	35.6
Air	1.76 ± 0.47	0.70 ± 0.19	8.1	55.0	3.02 ± 0.08	1.20 ± 0.03	1.7	11.8

*Charges fired at a scaled height of 0.5 ft lb$^{-1/3}$ or 0.20 m kg$^{-1/3}$ above the snow surface.

in, the snow cover. The pressure values, however, are from transducers on the surface of the snow and cannot be used to estimate the attenuation coefficient of the snow itself. He observed that peak amplitudes attenuated more rapidly in wet snow than in dry snow and that plastic deformation occurred 1 to 1.5 m from a 1-kg charge buried in the snow. This corresponds to an effective scaled radius of 1 to 1.5 m kg$^{-1/3}$, in agreement with the value of 1.6 m kg$^{-1/3}$ obtained from Livingston's data.

Summary of snow experiments

To summarize the experimental work on snow, laboratory measurements have determined only the broad outlines of the dynamic behavior of snow. Napadensky's (1964) data give the general relationship between wave and particle velocity, but an improved theory is needed to convert these measured values to pressures and densities. Sato and Wakahama's (1976) study revealed qualitative information on the mechanism of snow deformation caused by an impact and showed that crack formation becomes important when the density of the snow approached 600 kg m^{-3}. Repeating these laboratory measurements with instruments giving increased resolution and with the measurement of as many parameters as possible (including wave and particle velocity, pressure, and final sample density) would be worthwhile. The field measurements of Livingston (1964) and of Wisotski and Snyder (1966) show that explosive charges fired in the snow produce stronger plastic waves than charges fired in the air. Livingston's (1964) data show that charges fired in Greenland snow have an effective scaled radius for plastic deformation of 1.6 m kg$^{-1/3}$ while charges fired in the air have an effective scaled radius of 1.2 m kg$^{-1/3}$. These trends were confirmed for seasonal snow by Wisotski and Snyder (1966) and by Gubler (1977).

Theoretical studies

Most of the theoretical work on inelastic stress wave propagation in snow has been done by Brown (1979a, b, 1980a, b). A review of this work is provided below.

Brown (1979a) applied Carroll and Holt's (1972) model to snow. The model of Carroll and Holt assumes a spherical, unconnected pore geometry and also presupposes that an applied compressive force causes compaction solely by decreasing the volume of the pores, with no reduction in the volume of the matrix material. Carroll and Holt also assumed a constant yield stress, $Y = Y_0$, defined using the von Mises criterion, for the matrix material. Brown (1979a) follows Carroll and Holt's derivations closely, the principal change being the substitution of a rate-dependent yield stress:

$$Y = S_0 + C \ln (AD) \tag{8}$$

where D = the principal difference of the rate of deformation tensor and where S_0, C, and A are arbitrary constants. Brown arrives at the plastic phase equation

$$P(t) = \frac{1}{3} \ln \left(\frac{\alpha}{\alpha-1}\right) \left[2(S_0-C) + C \ln \frac{(-\dot{\alpha}A^2)}{\alpha(\alpha-1)}\right] - \rho_{ice} (\psi_b - \psi_a) \tag{9}$$

where $\alpha = \rho_{ice}/\rho$, and the last term in eq 9 represents an acceleration. The acceleration term is dropped for the remainder of the 1979a paper since cases at low rates of deformation are being investigated. A work-hardening factor of $J\, e^{-\phi\alpha/\alpha_0}$ is also added to the equation. J and ϕ are additional empirically determined material constants, and the subscript zero refers to the initial state.

In Brown (1980a), eq 9 is stated as

$$\dot{P}(t) = \frac{P}{\alpha} = \frac{J}{3\alpha} \ln \left(\frac{\alpha}{\alpha-1}\right) \left[2(S_0 - C) + C \ln \frac{(-\dot{\alpha}A^2)}{\alpha(\alpha-1)}\right] - \frac{\tau^2}{2\alpha} \frac{d}{d\alpha} [\dot{\alpha}^2 f(\alpha)] \tag{10}$$

where

$\tau^2 = \rho_{ice}\, a_0^2/3(\alpha_0 - 1)$,

$f(\alpha) = (\alpha - 1)^{-1/3} - \alpha^{-1/3}$,

a_0 = the initial average pore radius

$\dot{P} = P/\alpha$.

For large rates of compaction, Brown assumes that the yield stress of ice is nearly constant, i.e.

$$Y = S_0$$

and finds

$$\dot{P}(t) = \frac{2JS_0}{3\alpha} \ln \left(\frac{\alpha}{\alpha-1}\right) e^{-\phi\alpha/\alpha_0} - \frac{\tau^2}{2\alpha} \frac{d}{d\alpha} [\dot{\alpha}^2 f(\alpha)]\,. \tag{11}$$

For these same conditions, Carroll and Holt (1973) derived the equation

$$\dot{P}(t) = \frac{P}{\alpha} = -\frac{1}{\alpha} \frac{d}{d\alpha} \frac{2}{3} Y [H(\alpha_2) - H(\alpha)] + \frac{\tau^2}{2} Y \dot{\alpha}^2 f(\alpha) \tag{12}$$

with

$$H(\alpha) = \alpha \ln \alpha - (\alpha - 1) \ln (\alpha - 1)\,.$$

and where α_2 is the value of α at the transition from elastic to plastic deformation. Performing the derivative with respect to α on the first term of eq 12 gives

$$\dot{P}(t) = \frac{2}{3\alpha} Y \ln \left(\frac{\alpha}{\alpha-1}\right) - \frac{\tau^2}{2\alpha} Y \frac{d}{d\alpha} [\dot{\alpha}^2 f(\alpha)] \tag{13}$$

which is the same as Brown's equation except for the work-hardening factor.

After obtaining eq 13, Carroll and Holt (1973) derive the equation for a stress wave propagating in the porous medium. They obtain

$$\Delta\dot{P} = -\frac{\rho_0}{\alpha_0} C_0^2 \;\Delta\alpha \tag{14}$$

for steady waves propagating with velocity C_0. Equation 14 depends on the assumption that the material behaves as a fluid. Although Carroll and Holt derive eq 14 in a general manner, it can be derived formally from eq 1 and 2 of this report with the notational change $U = C_0$. The theory ignores fracture formation. Since fracturing occurs in snow when the predicted final density is 600 kg m^{-3} or larger, the theory will have to be modified to be applicable to snow in this range. Substituting eq 11 into 14, Brown (1979a) obtains

$$\Delta\hat{P} = -\frac{1}{\alpha_0}\rho_0 C_0^2 (\alpha - \alpha_0) = \frac{2S_0}{3\alpha} J \ln\left(\frac{\alpha}{\alpha - 1}\right) e^{-\phi\alpha/\alpha_0} - \frac{\tau^2 C_0^2}{2\alpha}\frac{d}{d\alpha}\left[\dot{\alpha}^2 f(\alpha)\right] \tag{15}$$

for shock waves in snow. By substituting values of the material constants S_0, J, and ϕ for single-crystal ice and integrating from α_0 to α, eq 15 is then used by Brown to evaluate the shock wave parameters in snow. For steady waves, $\dot{\alpha} = 0$ and the result is

$$\begin{aligned}\Delta\hat{P} = 2S_0 J \left[\alpha^2 - \frac{1}{2}\alpha_0(\alpha + \alpha_0)\right]^{-1} \Bigg\{ & -\frac{\alpha_0}{\phi}\left[e^{-\phi\alpha/\alpha_0}\ln\alpha - e^{-\phi}\ln\alpha_0 - \ln\frac{\alpha}{\alpha_0}\right. \\ & \left. - \sum_{n=1}^{\infty}\frac{(-\phi)^n}{n \cdot n!}\left(\left(\frac{\alpha}{\alpha_0}\right)^n - 1\right)\right] + e^{-\phi/\alpha_0}\frac{\alpha}{\phi}\left[e^{-\phi(\alpha-1)/\alpha_0}\ln(\alpha-1) - e^{-\phi(\alpha_0-1)/\alpha_0}\ln(\alpha_0-1)\right. \\ & \left. - \ln\left(\frac{\alpha-1}{\alpha_0-1}\right) - \sum_{n=1}^{\infty}\frac{(-\phi)^n}{n \cdot n!}\left(\left(\frac{\alpha-1}{\alpha_0}\right)^n - \left(\frac{\alpha_0-1}{\alpha_0}\right)^n\right)\right]\Bigg\}. \end{aligned} \tag{16}$$

Equation 16 gives the pressure change caused by the passage of a wave compacting the snow from α_0 to α. This pressure depends on the density change (given by α_0 and α), the yield stress S_0 of ice, and the empirical work-hardening factors J and ϕ. The equation is subject to the same limitation as eq 14, i.e. fractures are neglected. Brown (1980b, c) derives similar equations for very low density snow, based on a different pore collapse mechanism.

Confirmation of the theory

Two procedures can be used to confirm the applicability of eq 16 to shock waves in snow. The first procedure is to qualitatively assess whether the model itself agrees with the actual behavior of snow; that is, it should be determined whether a compaction of snow does indeed occur because of a compaction of the pore spaces only, or whether additional processes are involved.

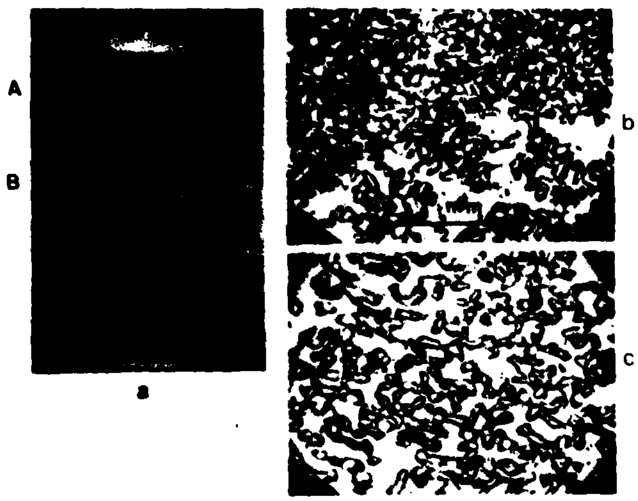

Figure 9. Snow thin sections. (a) Thin section through snow deformed by the impact of a falling weight. (b) Thin section from the boundary between compacted portion (A) and undisturbed portion (B) of snow. (c) Thin section of undisturbed portion of snow. Reproduced from Sato and Wakahama (1976).

Sato and Wakahama (1976) show a thin section of snow deformed by the impact of a falling weight (reproduced in Fig. 9). The final density is not given, but since no large fractures are visible in the figure, it is probably less than 600 kg m^{-3}. The thin section shows that the pores are indeed compressed by the impact. However, the figure also shows that the pores are neither spherical nor isolated from one another as assumed in Carroll and Holt's theory, and the average grain size also decreases after the impact due to fracturing of the grains themselves. Both of these observations require modification of the theory to accurately represent the physical behavior of snow.

The second method of confirming the theory is to compare the predictions of eq 16 with measurements on snow. This comparison would also allow the choice of material coefficients to be verified.

Brown (1979a) chose values of $J = 3.07$ and $\phi = 5.28$ by fitting the model predictions to data from Abele and Gow (1976). The yield stress $Y \simeq S_0$ at high strain rates was given a value of 3×10^7 N m^{-2}. This value seems very high as it implies a strain rate of 2×10^5 s^{-1}. Since the yield strength is a simple multiplier in eq 16, a change in this factor would produce a proportional change in the observed pressure P for a given compaction $\Delta\alpha$. Brown (1979b, 1980a) compared the predictions of eq 16 to the data of Napadensky (1964). However, because of the problems associated with Napadensky's experiment, a comparison with these data is not sufficient to confirm the theory. Figure 5 shows a comparison of Napadensky's actual measurements with Brown's (1980a) predicted values.

Discussion

Brown (1980a) states that Napadensky's data at lower amplitudes are questionable because, when extrapolated as on Brown's Figure 2, they predict a decrease to zero in the wave velocity whereas an elastic wave velocity is expected. However, it is not necessarily the data that are incorrect. First, Napadensky's data relate to high pressures where only a plastic wave exists (see Fig. 1). These data cannot be extrapolated to lower pressures since a substantial change in material behavior is expected. Second, the theory itself predicts that the *plastic* wave velocity will decrease. As the pressure (or wave amplitude) decreases, two waves will exist, a precursor elastic wave and a plastic wave. With a further decrease in pressure (below the elastic limit) only an elastic wave will be produced and it will propagate at the elastic wave speed. The plastic wave velocity behind it will decrease towards zero, so the data cannot be questioned on those grounds. Since the elastic wave velocity is an order of magnitude higher (1.9 km s^{-1} for snow of 500-kg m^{-3} density) than any velocity shown in Brown's Figure 2, it would take an extreme extrapolation to enable either the theoretical or the experimental data to achieve this value at the intercept.

Carroll and Holt's (1972) theory, applied to snow by Brown (1979a), is the first attempt to account for the compressibility of snow in predicting its response to stress waves. However, there are a number of conceptual problems with the application of this model to snow. As mentioned above, the pores in snow are not spherical nor isolated as the theory assumes. This observation would require some changes to the theory, and Brown (1980b) has made some geometric changes in his paper on low density snow. However, a number of empirical factors were added to the derived equations to allow a good fit to experimental results.

A more serious objection to the theory is that pore compaction alone will not account for the compression of snow to solid ice at high strain rates. The observations of Sato and Wakahama (1976) show that the dominant mechanism of deformation will change after a density of about 600 kg m^{-3} is reached. If the theory is applied only to compactions to 600 kg m^{-3} or less, major changes in the calculated parameters of the stress waves in snow occur. The most serious drawback to the theory is the failure to account for the fracturing of bonds in the snow. Figure 9 clearly shows that grains have been fractured by an impact, yet the theory of Carroll and Hold assumes that all deformations will occur plastically (by flowing rather than fracturing). Seaman et al. (1974) briefly discuss some of the modifications necessary to account for fracturing.

The spherical pore model applied to snow by Brown (1979a) is the first attempt to mechanistically model the deformation caused by the propagation of inelastic stress waves through snow. The model may be applicable to small deformations, but experimental data are needed for its confirmation in this range. Because of conceptual problems, the model requires extensive modifications to correctly describe large deformations.

APPLICATIONS

In this section the problem of determining the amplitude of a pressure wave in snow caused by an explosion above the snow is investigated. This problem is of interest because of applications in clearing a snow-covered minefield and in controlling the release of avalanches.

Brown (1979b) applied a finite-difference calculation to eq 16 to find the attenuation of a pressure wave as a function of depth propagated into snow. The snow was assumed to have an initial density of 350 kg m^{-3}. For a plane wave with a peak pressure of 2100 kPa at the surface, Brown's calculations showed that the pressure decreased to 400 kPa at 0.05-m depth and to 100 kPa at 0.40-m depth (Brown 1979b, Fig. 9). The calculated density changes at these depths were 110 kg m^{-3} and less than 50 kg m^{-3}, respectively.

The calculations of Brown (1979b) agree fairly closely with data from Wisotski and Snyder (1966) as shown in Brown's Figure 9. The agreement is not as close when compared to Livingston's (1964) results (see Table 2). Aside from the experimental scatter, some of the differences in the data can be attributed to the higher initial snow density for Livingston's experiments. In addition, both of the measured data sets show the attenuation of a spherical wavefront from a point source rather than the plane wave attenuation calculated by Brown. The calculations and the data are qualitatively in agreement in showing a very large decrease in amplitude as the wave travels through the snow.

Table 2. Pressure vs distance for a 1-lb explosive charge fired in snow.

d (m)	λ ($m\ kg^{-1/3}$)	P_1* (kPa)	P_2† (kPa)
0.46	0.60	664	951
0.61	0.80	161	371
0.76	0.99	13.1	179
0.91	1.19	3.2	98.1
1.37	1.79	9.2	25.1
1.52	1.98	5.6	17.8
1.83	2.39	1.5	9.6
5.49	7.16	0.6	0.2

*Pressures measured by Wisotski and Snyder (1966). Converted from psi to kPa from their Table A-6.
†Pressures calculated using eq 7 and coefficients found from Livingston's (1964) data.

Brown's calculations give final density values of 590 kg m^{-3} at the surface and 410 kg m^{-3} at a depth of 0.1 m. These values are lower than those usually observed in the crater region (600 kg m^{-3}, Livingston 1968). Thus some of Brown's calculated results are questionable because they give a higher attenuation rate for plane waves than the rate measured for spherical wavefronts, and since very little compaction of the snow is predicted. These discrepancies point out the need for further experimental measurements and for extending the theory to take fractures into account.

Table 3. Maximum effective radius for clearing mines as a function of charge size. Charges were fired in the air.

Charge size (lb)	*Charge size (kg)*	*Maximum effective radius (m)*
1	0.5	0.6
5	2.3	1.1
10	4.6	1.3
40	18.2	2.2
100	45.5	3.0
500	227.3	5.1

Dennis (1973) provides data that can be used to assess the effect of snow cover on clearing a minefield. Dennis shows that overpressures of 100 to 320 kPa are needed to set off various U.S. (and one Soviet) mines. These pressure ranges are all within the true crater zone for snow; thus for shallowly buried mines the maximum effective (mine clearing) radius will always be less than the true crater radius. For a charge fired in the air, an overpressure of 320 kPa will be produced at a reduced distance of 0.83 m $kg^{-1/3}$ (using the coefficients from Livingston's 1964 data). The mine clearing radius for various charge sizes is listed in Table 3. Use of a fuel-air explosive (FAE) will increase this radius significantly because the size of the source region is increased and because the shock wave is plane rather than spherical. Dennis (1973, Fig. 60) shows that the 345-kPa zone of overpressure extends about 10 m from the center of a FAE. For shallowly buried mines the effective clearing radius could be expected to extend this far.

These estimates are not very satisfying, since they only give a maximum effective radius. The actual clearing radius will decrease as the thickness of the snow layer increases because of further attenuation of the shock wave by the snow. In addition, the question of how an inelastic wave in snow interacts with a mine fuze has been completely ignored. Some losses are expected (i.e. not all of the pressure will be transmitted to the mine because of an impedance mismatch) but no estimate of the effect can be given as no measurements have been made.

RECOMMENDATIONS

At present, the best approach for assessing the influence of a snow layer on the use of an explosion in the air to clear a minefield is to test the method directly; that is, to field test the method with live or dummy instrumented mines beneath a snow layer. The advantages of such a test are that it avoids the difficulties in calculating the response of snow to large deforming overpressures and in estimating the coupling effects at the air/snow and snow/mine interfaces. If care is given to the experimental arrangement and if calibrated gauges are used, these tests could also provide needed experimental information on the response of snow itself to such large overpressures.

In general, basic theoretical and experimental work on snow is still very much needed. The spherical pore model applied to snow by Brown (1979a) contains some basic conceptual drawbacks as pointed out above. Another approach, starting perhaps from the model of grains in contact, will need to be used. In addition, the experimental work of Sato and Wakahama (1976) has shown that any model will have to account for fracture effects to explain large deformations of snow.

More experimental data are also needed. Since the dynamic response of snow is poorly understood at present, these data should be obtained before further theoretical work is done. Experiments involving the use of multiple gauges are probably a suitable approach. These measurements should first be done on sifted snow in the laboratory to characterize the general dynamic compaction behavior. Later, the measurements can be done in situ or on natural snow samples to determine the variability in behavior due to density variations, thawed layers, etc.

SUMMARY

Experimental and theoretical work on inelastic stress wave propagation in snow has been reviewed. The work of Abele and Gow (1976) shows that snow is a viscoplastic material capable of supporting the propagation of elastic and plastic waves, but not supersonic shock waves. Napadensky's (1964) study gives only the relation between wave and particle velocity caused by an impact, since the hydrodynamic theory is invalid for these data and cannot be used to convert the measured values to pressures and densities. Sato and Wakahama's (1976) experiments give qualitative information on the deformation mechanism in snow, but additional laboratory work is needed. Explosion tests by Livingston (1964) and Wisotski and Snyder (1966) have been analyzed and show that charges fired in the snow produce larger plastic waves than charges fired in the air. The effective scaled radius for plastic deformation is 1.6 m $kg^{-1/3}$ for charges fired in the snow and 1.2 m $kg^{-1/3}$ for charges fired in the air.

Carroll and Holt (1972, 1973) have developed a theory of compaction for impermeable porous materials. By considering the matrix material to be ice, the theory has been used by Brown (1979a, 1980a) to predict the behavior of snow to shock wave loading. There are conceptual problems in the applicability of this theory to snow, and accurate experimental data are needed to assess the utility of this model. Additional theoretical development is also needed to account for the fracturing that occurs in compressing snow to high densities at high strain rates.

LITERATURE CITED

Abele, G. and A.J. Gow (1976) Compressibility characteristics of compacted snow. CRREL Report 76-21. ADA028622.

Brown, R.L. (1979a) A volumetric constitutive law for snow subjected to large strains and strain rates. CRREL Report 79-20. ADA075474.

Brown, R.L. (1979b) An analysis of plastic shock waves in snow. CRREL Report 79-29. ADA080051.

Brown, R.L. (1980a) Pressure waves in snow. *Journal of Glaciology*, **25**: 99-107.

Brown, R.L. (1980b) A volumetric constitutive law for snow based on a neck growth model. *Journal of Applied Physics*, **51**: 161-165.

Brown, R.L. (1980c) Propagation of stress waves in alpine snow. *Journal of Glaciology*, **26**: 235-243.

Butcher, B.M., M.M. Carroll and A.C. Holt (1974) Shock-wave compaction of porous aluminum. *Journal of Applied Physics*, **45**: 3864-3875.

Carroll, M.M. and A.C. Holt (1972) Static and dynamic pore-collapse relations for ductile porous materials. *Journal of Applied Physics*, **43**: 1626-1636.

Carroll, M.M. and A.C. Holt (1973) Steady waves in ductile porous solids. *Journal of Applied Physics*, **44**: 4388-4392.

Carroll, M.M. (1980) Compaction of dry or fluid-filled porous materials. *Journal of the Engineering Mechanics Division, ASCE*, **106**: 969-990.

Dennis, J.A. (1973) Results of variable parameters on the blast effects of Navy BLU-73/B, fuel air explosive (FAE) warheads. USA MERDC Report 1071. AD527019L.

Duvall, G.E. and G.R. Fowles (1963) Shock waves. In *High Pressure Chemistry and Physics*, (R.S. Bradley, Ed.), New York: Academic Press, 2: 209-291.

Eisenberg, M.A. (1980) *Introduction to the mechanics of solids.* Reading, Massachusetts: Addison-Wesley.

Fowles, G.R. (1961) Shock wave compression of hardened and annealed 2024 aluminum. *Journal of Applied Physics*, **32**: 1475–1487.

Gubler, H. (1977) Artificial release of avalanches by explosives. *Journal of Glaciology*, **19**: 419–429.

Ingram, L.F. (1960) Blast effects on a snow tunnel, Camp Century, Greenland. USAE Waterways Experiment Station MP 2-378.

Ingram, L.F. and J.N. Strange (1958) Blast-pressure measurements in snow. USAE Waterways Experiment Station MP 2-274.

Joachim, C.E. (1967) Shock transmission through ice and snow. USAE Waterways Experiment Station Technical Report 1-794.

Kolsky, H. (1963) *Stress waves in solids.* New York: Dover Publications.

Livingston, C.W. (1968) Explosions in snow. CRREL Technical Report 86.

Livingston, C.W. (1964) Explosions in snow. CRREL Internal Report 37 (unpublished).

Love, A.E.H. (1944) *A Treatise on the Mathematical Theory of Elasticity.* New York: Dover Publications.

Mellor, M. (1964) Properties of snow. CRREL Monograph III-A1. AD611023.

Mellor, M. (1965) Explosions and snow. CRREL Monograph III-A3a. AD623418.

Mellor, M. (1975) A review of basic snow mechanics. International Association of Hydrological Sciences Publication No. 114, p. 251–91.

Napadensky, H. (1964) Dynamic response of snow to high rates of loading. CRREL Research Report 119. AD600075.

Napadensky, H.S. (1965) Shock waves in arctic snow. Final report on Illinois Institute of Technology Research Institute Project T6041, Contract No. DA-27-021-AMC-8(X) (unpublished).

Poulter, T.C. (1950) Geophysical studies in the Antarctic. Stanford Research Institute, Stanford, California.

Sato, A. and G. Wakahama (1976) Plastic wave in snow. *Low Temperature Science*, Ser A, **34**: 59–69 (in Japanese, with English summary). Published in English as G. Wakahama and Sato, A. (1977) Propagation of a plastic wave in snow. *Journal of Glaciology*, **19**: 175–183.

Schatz, J.F. (1976) Models of inelastic volume deformation for porous materials. In: *The Effects of Voids on Material Deformations* (S.C. Cowin and M.M. Carroll, Eds.) Applied Mechanics Division of the ASME, New York, p. 141–170.

Seaman, L. (1976) An evaluation of dynamic experimental methods for porous materials. In *The Effects of Voids on Material Deformations* (S.C. Cowin and M.M. Carroll, Eds.), Applied Mechanics Division of the ASME, New York, p. 141–170.

Seaman, L., R.E. Tokheim and D.R. Curran (1974) Computational representation of constitutive relations for porous material. Stanford Research Institute Report DNA 3412. ADA007921.

Smith, J.L. (1969) Shock tube experiments on snow. CRREL Technical Report 218. AD692291.

Swegle, J.W. (1980) Constitutive equation for porous materials with strength. *Journal of Applied Physics*, **51**: 2574–2580.

Wisotski, J. and W.H. Snyder (1966) A study of the effects of snow cover on high explosive blast parameters. University of Denver–Denver Research Institute Final Report on Contract N60921-7016.

APPENDIX A. SELECTED DATA FROM WISOTSKI AND SNYDER (1966).

Table A-1. Selected pressure data from Wisotski and Snyder (1966).

Distance	Charge fired in air				Charge fired in snow			
	Pressure in snow		Pressure in air††		Pressure in shallow snow†		Pressure in deep snow***	
(ft)	(psi)	(kPa)	(psi)	(kPa)	(psi)	(kPa)	(psi)	(kPa)
0.5	10.08 ± 2.84 (3)*	70.41 ± 19.84						
1.5	1.38 ± 0.81 (2)*	9.64 ± 5.7			37.5	262	96.3	673
2.0					13.7	95.7	23.4	163
2.5	0.36 ± 0.36 (3)*	2.5 ± 2.5					1.9	13
3.0					1.02	7.12	0.47	3.3
4.5					0.37	2.6	1.34	9.36
5.0	2.18 ± 0.81 (5)††	15.2 ± 5.7	37.0 ± 1.7 (3)	258 ± 12			0.81	5.7
6.0							0.21***	1.5
8.0	1.68 ± 0.56 (14)††	11.7 ± 3.9	11.50 ± 0.87 (11)	80.3 ± 6.1				
12.0	1.71 ± 0.92 (12)††	11.9 ± 6.4	5.91 ± 2.61 (10)	41.3 ± 18.2				

Numbers in parentheses are number of data points used in calculation of average values and standard deviations. All measurements used paddle gauges unless otherwise noted.

* Average and standard deviation calculated for shots 63–65 from Wisotski and Snyder's (1966) Table A-8. Charge was 2 ft above snow surface.

† Average peak pressure at mid-depth in snow from charges fired within snow. Average snow depth 15.9 in., average snow density 252 kg m^{-3}. Values reproduced from Wisotski and Snyder's (1966) Table A-5.

** Same as note 2 except average snow depth 36 in. and average snow density 262 kg^{-3}. Values reproduced from Wisotski and Snyder's (1966) Table A-6.

†† Average and standard deviation calculated from Wisotski and Snyder's (1966) Table A-4.

*** Pencil gauge measurement.

PREVIOUS PAGE IS BLANK

APPENDIX B. PRESSURE DATA FROM LIVINGSTON (1964).

Tables B1-B3 contain pressure data for 36 shots from Livingston (1964). Gauge locations are shown in Figures 20-24 in Livingston (1968). Pressures outside the stated calibrated gauge ranges have been omitted. These gauge pressure ranges are (Livingston 1968):

Water-shock gauge	30-3000 psi	(0.21-20.7 MPa)
Baffle gauge	5-30 psi	(34.5-207 kPa)
Pencil gauge	0.4-6 psi	(2.8-41.4 kPa)

Data are listed by charge location: in the snow, on the surface, and in the air. Pressures have been converted from psi to kPa and lengths from ft to m.

Figure B1 shows the relationship between pressure and reduced distance for surface explosions. Table B4 gives the coefficients found by fitting the data to eq 7 of the text.

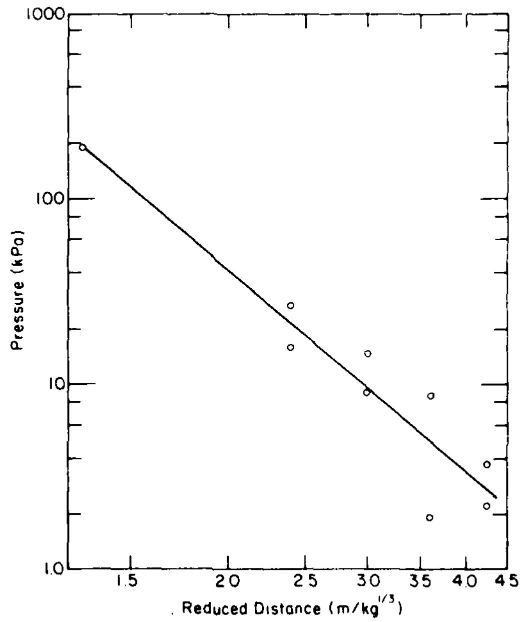

Figure B1. Graph of log of maximum pressure vs log reduced distance for explosions on the surface of Greenland snow. Data from Livingston (1964).

PREVIOUS PAGE IS BLANK

Table B1. Charges fired in snow (83 pressure measurements).

Charge (kg)	Charge root ($kg^{1/3}$)	Distance (m)	Reduced distance ($m\ kg^{-1/3}$)	Log of distance	Pressure (kPa)	Log of pressure
1.14	1.04	1.01	0.97	-0.01	1020.42	3.01
1.14	1.04	1.29	1.24	0.09	827.36	2.92
1.14	1.04	1.29	1.24	0.09	155.13	2.19
1.14	1.04	2.12	2.03	0.31	19.99	1.30
1.14	1.04	3.57	3.42	0.53	6.21	0.79
2.27	1.31	0.52	0.40	-0.40	8011.64	3.90
2.27	1.31	0.78	0.59	-0.23	2392.46	3.38
2.27	1.31	1.12	0.85	-0.07	91.70	1.96
2.27	1.31	1.56	1.19	0.08	39.30	1.59
2.27	1.31	2.35	1.79	0.25	6.89	0.84
2.27	1.31	3.39	2.58	0.41	4.14	0.62
4.55	1.66	0.66	0.40	-0.40	2930.25	3.47
4.55	1.66	0.98	0.59	-0.23	1689.20	3.23
4.55	1.66	1.41	0.85	-0.07	703.26	2.85
4.55	1.66	1.41	0.85	-0.07	142.03	2.15
4.55	1 66	1.97	1.19	0.07	39.99	1.60
4.55	1.66	4.24	2.56	0.41	16.55	1.22
4.55	1.66	0.98	0.55	-0.23	1675.41	3.22
4.55	1.66	4.26	2.57	0.41	8.96	0.95
18.18	2.63	1.56	0.59	-0.23	1551.31	3.19
18.18	2.63	2.24	0.85	-0.07	322.67	2.51
18.18	2.63	6.77	2.57	0.41	13.10	1.12
18.18	2.63	1.56	0.59	-0.23	868.73	2.94
18.18	2.63	2.24	0.85	-0.07	295.78	2.47
18.18	2.63	4.69	1.78	0.25	9.65	0.98
18.18	2.63	6.78	2.58	0.41	9.65	0.98
1.14	1.04	0.72	0.69	-0.16	4584.97	3.66
1.14	1.04	1.29	1.24	0.09	382.66	2.58
1.14	1.04	1.29	1.24	0.09	115.83	2.06
1.14	1.04	2.29	2.20	0.34	54.47	1.74
1.14	1.04	2.12	2.03	0.31	17.93	1.25
1.14	1.04	3.57	3.42	0.53	11.03	1.04
2.27	1.31	0.52	0.40	-0.40	2254.57	3.35
2.27	1.31	0.78	0.59	-0.23	737.78	2.87
2.27	1.31	1.12	0.85	-0.07	202.01	2.31
2.27	1.31	1.12	0.85	-0.07	59.98	1.78
2.27	1.31	1.56	1.19	0.08	35.85	1.55
2.27	1.31	2.35	1.79	0.25	16.55	1.22
2.27	1.31	3.39	2.58	0.41	6 89	0.84
4.55	1.66	0.66	0.40	-0.40	2254.57	3.35
4.55	1.66	0.98	0.59	-0.23	937.68	2.97
4.55	1.66	1.41	0.85	-0.07	626.73	2.80
4.55	1.66	2.62	1.58	0.20	153.75	2.19
4.55	1.66	4.25	2.57	0.41	2.76	0.44
4.55	1.66	0.98	0.59	-0.23	470.91	2.67
4.55	1.66	1.41	0.85	-0.07	115.83	2.06
4.55	1.66	1.97	1.19	0.07	62.74	1.80
4.55	1.66	4.26	2.57	0.41	9.65	0.98
18.18	2.63	1.56	0.59	-0.23	1330.68	3.12
18.18	2 63	2.24	0.85	-0.07	153.06	2.18
18.18	2.63	6.77	2.57	0.41	2.76	0.44
18.18	2.63	1.56	0.59	-0.23	944.57	2.98
18.18	2.63	2.24	0.85	-0.07	224.08	2.35
18.18	2.63	2.24	0.85	-0.07	117.21	2.07
1.14	1.04	3.73	0.70	-0.16	3199.14	3.51
1.14	1.04	1.01	0.57	-0.01	703.26	2.85
1.14	1.04	1.29	1.24	0.05	166.16	2.22
1.14	1.04	3.57	3.42	0.53	4.14	0.62

Charge (kg)	Charge root ($kg^{1/3}$)	Distance (m)	Reduced distance ($m\ kg^{-1/3}$)	Log of distance	Pressure (kPa)	Log of pressure
2.27	1.31	2.52	0.40	-0.49	5046.92	3.70
2.27	1.31	3.78	0.59	-0.23	2192.51	3.34
2.27	1.31	1.12	0.85	-0.07	602.60	2.78
2.27	1.31	1.12	0.85	-0.07	55.16	1.74
2.27	1.31	2.35	1.75	0.25	6.85	0.84
2.27	1.31	3.39	2.58	0.41	2.76	0.44
4.55	1.66	3.66	3.40	-0.40	5412.34	3.73
4.55	1.66	3.96	0.59	-0.23	1378.94	3.14
4.55	1.66	1.41	0.85	-0.07	512.97	2.71
4.55	1.66	1.41	0.85	-0.07	43.44	1.64
4.55	1.66	1.97	1.19	0.07	50.33	1.70
4.55	1.66	2.62	1.58	0.20	46.88	1.67
4.55	1.66	2.62	1.58	0.20	28.27	1.45
4.55	1.66	4.22	2.35	0.41	6.21	0.79
4.55	1.66	0.39	0.59	-0.23	673.81	2.83
4.55	1.66	1.41	0.85	-0.07	155.13	2.19
4.55	1.66	2.95	1.78	0.25	15.86	1.20
18.18	2.63	1.56	0.59	-0.23	1110.05	3.05
18.18	2.63	2.24	0.85	-0.07	252.35	2.40
18.18	2.63	2.24	0.85	-0.07	183.40	2.26
18.18	2.63	6.77	2.57	0.41	13.79	1.14
18.18	2.63	1.56	0.59	-0.23	799.79	2.90
18.18	2.63	2.24	0.85	-0.07	142.72	2.15
18.18	2.63	4.69	1.78	0.25	17.93	1.25
18.18	2.63	6.78	2.58	0.41	5.52	0.74

Table B2. Charges fired on surface of snow (9 pressure measurements).

Charge (kg)	Charge root ($kg^{1/3}$)	Distance (m)	Reduced distance ($m\ kg^{-1/3}$)	Log of distance	Pressure (kPa)	Log of pressure
4.55	1.66	1.64	0.99	-0.01	183.40	2.26
4.55	1.66	1.64	0.99	-0.01	109.63	2.04
4.55	1.66	1.96	1.18	0.07	62.05	1.79
4.55	1.66	2.29	1.38	0.14	13.10	1.12
4.55	1.66	2.63	1.59	0.20	15.17	1.16
4.55	1.66	2.63	1.59	0.20	25.51	1.41
4.55	1.66	0.98	0.59	-0.23	1316.89	3.12
4.55	1.66	1.97	1.19	0.07	101.35	2.01
4.55	1.66	2.29	1.38	0.14	59.98	1.78

Table B3. Charges fired in air.

Charge (kg)	Charge root ($kg^{1/3}$)	Distance (m)	Reduced distance ($m\ kg^{-1/3}$)	Log of distance	Pressure (kPa)	Log of pressure
4.55	1.66	1.07	0.64	-0.19	79.29	1.90
4.55	1.66	1.07	0.64	-0.19	33.78	1.53
4.55	1.66	1.07	0.64	-0.19	70.33	1.85
4.55	1.66	1.12	0.68	-0.17	142 72	2.15
4.55	1.66	1.12	0.68	-0.17	99.97	2.00
4.55	1.66	1.36	0.82	-0.09	62.74	1.80
4.55	1.66	1.36	0.82	-0.09	34.47	1.54
4.55	1.66	1.36	0.82	-0.09	35.16	1.55
4.55	1.66	1.36	0.82	-0.09	17.24	1.24
4.55	1.66	1.72	1.04	0.02	17.93	1.25
4.55	1.66	1.72	1.04	0.02	11.72	1.07
4.55	1.66	1.72	1 04	0.02	82.74	1.92
4.55	1.66	1.72	1.04	0.02	19.31	1.29
4 55	1.66	2.03	1.22	0.09	7.58	0.88
4.55	1.66	2.03	1.22	0.09	7.58	0.88
4.55	1.66	2.03	1 22	0.09	12.41	1.09
4.55	1.66	2.03	1.22	0.09	9.65	0.98
4.55	1.66	2.03	1.22	0.09	11.72	1.07
4.55	1.66	2.03	1.22	0.09	8.96	0.95
4.55	1.66	0.84	0.50	-0.30	85.49	1.93
4.55	1.66	1.46	0.88	-0.05	18.62	1.27

Table B4. Coefficients of eq 7 found from Livingston's (1964) data.

Charge location	N	C_1	C_3	MSE in pressure
Snow[1]	83	-3.33	5.50	0.301
Snow[2]			1.74×10^5	
Surface[1]	9	-4.34	11.20	0.149
Surface[2]			1.38	
Air[1]	21	-2.86	40.7	0.161
Air[2]			2.00×10^4	

N = number of data points
MSE = mean square error
1: Pressure in psi, λ in ft $lb^{-1/3}$.
2: Pressure in kPa, λ in m $kg^{-1/3}$.
Equation is

$$\log P = C_1 \log \lambda + C_2$$

A facsimile catalog card in Library of Congress MARC format is reproduced below.

Albert, Donald G.
Review of the propagation of inelastic pressure waves in snow / by Donald G. Albert. Hanover, N.H.: Cold Regions Research and Engineering Laboratory; Springfield, Va.: available from National Technical Information Service, 1983.
v, 33 p., illus.; 28 cm. (CRREL Report 83-13.)
Prepared for Office of the Chief of Engineers by Corps of Engineers, U.S. Army Cold Regions Research and Engineering Laboratory under DA Project 4A762730 AT42.
Bibliography: p. 18.
1. Explosives. 2. Fuel-air explosives. 3. Inelastic pressure waves. 4. Pressure signatures. 5. Snow. I. United States. Army. Corps of Engineers. II. Cold Regions Research and Engineering Laboratory, Hanover, N.H. III. Series: CRREL Report 83-13.